The Synthesis and Implementation of Pebax/PEG 400/NH₂-MIL125 Nanocomposite Membranes to Separate CO₂/CH₄

Cyrus Fallahi[1], Sadegh Moradi[2*], and Reza Mosayebi Behbahani[3]

[1] Ph.D. Candidate, Chemical Engineering Department, Faculty of Engineering, Arak University, Arak, Iran
[2] Assistant Professor, Chemical Engineering Department, Faculty of Engineering, Arak University, Arak, Iran
[3] Professor, Gas Engineering Department, Petroleum University of Technology, P.O. Box 63431, Ahwaz, Iran

Abstract

In the present study, the permeabilities of CO_2 and CH_4 in terms of ideal and actual CO_2/CH_4 selectivity were investigated through the synthesized membranes of poly (ether-block-amide) (Pebax 1657) accompanied with poly (ethylene glycol) (PEG 400) and NH_2-MIL125 nanoparticles. NH_2-MIL125 nanofillers were added to the blend of PEG 400 and Pebax 1657 at various weight fractions to fabricate polymeric nanocomposite membranes. Several analyses such as the crystalline structure of the synthesized membranes, field emission scanning electron microscopy (FESEM) and X-ray diffraction analysis (XRD) were utilized to investigate the cross-sectional and surface morphology of the membranes; the formation of the chemical bonds was identified by Fourier transform infrared (FTIR). This study presents the permeation of both pure and mixed gases of methane and carbon dioxide through Pebax 1657, Pebax/PEG blend, and the Pebax/PEG/NH_2-MIL125 nanocomposite membranes in a pressure range of 2-8 bar and at ambient temperature. The findings demonstrated that the synthesized nanocomposite membranes had a positive effect on the separation performance in comparison with the membranes made of neat polymer and polymer blends.

Keywords: CO_2/CH_4 Separation, Pebax 1657 Membrane, PEG, MOF, NH_2-MIL125 Nanoparticles

1. Introduction

The presence of carbon dioxide (CO_2) in natural gas, as one of the most significant challenges of industry, has negative effects on heating value and pipeline capacity (Adewole et al., 2015; Cong et al., 2012; Asadi and Ehsani, 2013; Ghaemi et al., 2017). CO_2 can be removed from natural gas using several conventional technologies, including absorption and cryogenic processes (Car et al., 2008b). However, the disadvantages of these technologies are high capital cost, a difficult process, and large space supplies. Consequently, implementing these technologies will be intensely limited in near future (Li and Chung, 2010). Therefore, it is a necessity to develop reliable techniques to reduce CO_2 emissions in industrial processes (Car et al., 2008a). Recently, membrane separation processes are considered as a promising alternative for CO_2 capture. They have several advantages such as small footprints, less capital investment, simplicity, lower energy consumption, lightness and compactness, insignificant influence on the environment, and skid mounted installation in comparison with pervious traditional processes (Azizi et al., 2017a). A proper selection of the membrane materials plays an important role in preparing a suitable membrane for a desire application. Currently, polymeric membranes are

---
* Corresponding Author:
    Email: s-morady@araku.ac.ir

considered as one of the best choices to capture CO_2 for many reasons such as their low cost, high process ability, and ease of preparation (Baker, 2002). There is a comprehensive study, presented by Lin and Freeman (2005), on the selection of membrane materials in order to reduce CO_2 from gas mixtures. Their results showed that the affinity of CO_2 to the polymer matrix was increased by the selection of polymers with polar groups. They have also concluded that the best polar group was ethylene oxide (EO) units to obtain higher values of CO_2 permeability and CO_2/light gas selectivity. Poly(ether-block-amide), as a member of the block copolymer family, is considered to be one of the good choices containing EO linkages. Pebax is a thermoplastic elastomer combining two parts of linear chains of polyether and the hard polyamide segments. Linear chains of polyether lead to high permeability, and hard polyamide segments renders mechanical strength (Flesher, 1986). In the present study, Pebax 1657 consisting of 40% amide segments and 60% ether segments is chosen as the polymer base for further modification. Figure 1 shows the chemical structure of Pebax 1657.
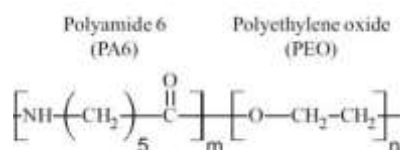

Figure 1
Chemical structure of Pebax 1657; weight ratio of PA6/PEO=40/60.

However, the use of polymeric membranes in the gas industry is limited by the inverse relationship between the permeability and selectivity (Robeson, 1991); therefore, polymeric membranes should be physically or chemically modified to increase both permeability and selectivity. Blend membranes show various effects on the gas transport properties by adding plasticizers (such as poly ethylene glycols (PEGs)) to the polymer matrix. PEG, as a very suitable plasticizer, is composed of EO units, which generally have a positive effect on the permeability of carbon dioxide and its selectivity towards nonpolar gases. The results of previous investigations indicated that lower molecular weight PEG led to a higher number of interactions between CO_2 molecules and polymer chain end groups. This can increase the solubility of CO_2 in PEG (Feng et al., 2013; Yang et al., 2012). Thus, PEG 400 has been employed to be blended with Pebax 1657 copolymer.

Nanoparticles also can be added into the polymer matrix, known as nanocomposite membranes, to increase the potency of polymeric membranes. Many researches have been conducted on the separation of CO_2/CH_4 by synthesizing Pebax 1657/PEG blend membranes (Car et al., 2008b; Car et al., 2008a; Habibzare et al., 2014; Azizi et al., 2017; Cho et al., 2014). However, the effects of simultaneously adding PEG and inorganic fillers into Pebax 1657 have been investigated in just few researches (Wang et al., 2014; Mahmoudi et al., 2015). Lately, a new class of microporous materials, known as metal organic frameworks (MOF's), have been considered as favorable fillers. According to gas separation, different types of MOFs such as ZIF-7, ZIF-8, ZIF-90, MIL-53, MIL-101, CuBTC, and CuTPA, UiO-66, UiO-67 have been utilized in membranes (Li et al., 2013; Naseri et al., 2015; Diestel et al., 2015). The polar functional groups such as -OH, -F, -SO_3H, -NH_2, and -COOH groups introduced onto aromatic rings in MOFs interact with CO_2 (Liu et al., 2013). A new titanium-based MOF MIL125 ($Ti_8O_8(OH)_4[O_2C$-C_6H_4-$CO_2]_6$), reported by Dan-Hardi et al. (2009), displays exceptional thermal stability and high porosity. Afterwards, Zlotea et al. (2011) introduced an amine-based MIL125 with more narrow spaces. The appearance of -OH radicals in polymeric clusters and -NH_2 radicals in linkers leads to the further separation of CO_2 from methane, as most studies pointed out (Moreira et al., 2012; Vaesen et al., 2013). CO_2 permeability can also be significantly improved by MOF particles with NH_2-

MIL125 fillers in membranes based on PSF and Matrimid® used for CH_4/CO_2 mixtures (Guo et al., 2015; Anjum et al., 2016).

Considering the effect of PEG and NH_2-MIL125 in CO_2 adsorption, Pebax/PEG/NH_2-MIL125 nanocomposite membranes have been modified to obtain higher values of CO_2 permeability and CO_2/CH_4 selectivity. To this end, PEG with a molecular weight of 400 was first added to Pebax 1657 which strongly bonds to acid gases. Then, the best blended Pebax/PEG membrane was modified by NH_2-MIL125 nanoparticles. Consequently, a solution blending method was employed to modify the structure of Pebax/PEG/NH_2-MIL125 nanocomposite membranes at different amounts of NH_2-MIL125 (4, 8, 12, and 16 wt.% Pebax and PEG). The optimum values of NH_2-MIL125 nanoparticles and PEG 400 were achieved to intensify CO_2 permeability at ideal and actual CO_2/CH_4 selectivity.

2. Experimental

2.1. Materials

Pebax® MH 1657 (consisting of 60 wt.% PEO and 40 wt.% PA6) was prepared from Arkema Inc. N,N-dimethylformamide (DMF) was used as solvent for nanocomposite membrane preparation; 2-aminoterephthalic acid (98%), methanol, PEG 400 (molecular weight of 400 g/mol), and n-hexane were provided by Merck Company. Pivalic acid (99%), terephthalic acid (98%), acetonitrile (99.8%), and tetraisopropyl orthotitanate (97%) were supplied by Sigma-Aldrich Company. CO_2, CH_4 pure (purity of 99.995%), and mixed CO_2/CH_4 (10/90 vol.%) gases were prepared from Sepehr Gas Kavian Company.

2.2. Synthesis of NH₂-MIL125 MOF's

MIL125 is typically synthesized by dissolving 17.5 g of pivalic acid in a solution of 5 ml of tetraisopropyl orthotitanate and 125 ml of acetonitrile (Frot et al., 2010). This solution is heated for 3-4 days at a temperature of 100 °C to obtain white crystals at a high yield. Then, a fine white powder is obtained by gently grinding the crystals, filtered off, and dried for 24 hours at a temperature of 80 °C. A mixture, composed of 50 ml DMF methanol (1:1), and 2.4 g of this powder is prepared and mixed with a solution containing 3 g terephthalic acid in 75 ml DMF. The prepared mixture is kept in an oven at 100 °C during 24 hrs. The excess of unreacted ligands is removed by washing the obtained powder with DMF. Then, MIL125 crystals are obtained by exchanging DMF with washing methanol. The same procedure was utilized to synthesize NH_2-MIL125 using different amounts of 2-aminoterephthalic acid (3.3 g) (Fu et al., 2012).

2.3. Membrane preparation

The solution casting method is used to prepare the membranes in this study. For preparation, the neat Pebax membrane, Pebax 1657, was dissolved in DMF under stirring for 3 hrs at 125 °C. The solution was then placed at 90 °C for 0.5 hrs to remove air bubbles. Afterwards, it was cast on a glass Petri dish and put in vacuumed oven at 80 °C for a day to evaporate its solvent. Finally, the membrane is detached from dish by normal hexane, and the residual solvent is removed from its structure by drying it in a vacuum oven at 50 °C for 5 hrs. In order to provide the desired membrane blends, different PEG 400 quantities, namely 0.1, 0.2, 0.3, and 0.4 wt.%, of Pebax 1657 are mixed with DMF while being stirred at ambient temperature for 1 hr. before it is added to the polymer. Next, the solution is stirred for 3 hrs at 125 °C. The membranes are cast and dried using a procedure similar to what is described earlier for the neat membrane. The procedure of preparing the nanocomposite membranes is as follows: first, different amounts (4, 8, 12, and 16 wt.% with respect to the blend polymers) of NH_2-MIL125

nanoparticles were mixed with DMF and sonicated for 1.5 hrs at 130 ° C. Afterwards, certain amounts of Pebax and PEG 400 are mixed with DMF during 1 hr. at 130 °C. NH_2-MIL125 nanoparticle solution were dispersed in the polymeric solution while stirring for 4 hrs at 130 °C. Petri dishes were used for the prepared solutions, and the membrane film was detached from the Petri dish and dried in the way discussed above. The dried membranes were cooled in ambient condition after being removed from the oven. Finally, these membranes were kept in a desiccator before usage.

3. MOF's particle and membrane characterization

3.1. Dynamic light scattering (DLS)

The DLS using a Malvern Instruments Model Number ZEN3600 (Scattering angle: 90°) is used to measure particle size distribution of NH_2-MIL125.

3.2. CO_2 adsorption analysis

CO_2 adsorption is carried out in order to characterize the textural properties of MOF's. Therefore, MICROMERITICS TRI STAR II PLUSE analyzer (USA) is applied after degassing the samples at 353 K for minimum 12 hrs under vacuum.

3.3. X-ray diffraction (XRD)

The X-ray diffraction tests are conducted by an ASENWARE, AW-XDM300 diffractometer. A Cu Kα source is embedded in the diffractometer to generate X-rays wavelength of 1.54184 Å. The range of diffraction angle (2θ) was from 5° to 90° to recognize crystal structure and intermolecular distances of intersegment chains.

3.4. Fourier transfer infrared spectroscopy (FTIR)

The Fourier transform infrared spectroscopy (FTIR) is applied using ALPHA FTIR spectrometer from Bruker. All spectra are developed from 4000 to 400 cm^{-1} under ambient conditions.

3.5. Field emission scanning electron microscopy (FESEM)

The field scanning electron microscopy (FESEM) is used to study the morphology of the prepared membranes. Sigma/Zeiss FESEM (Germany) is used in this study. It should be mentioned that, to analyze our synthesized membranes, they were coated with gold and fractured in liquid nitrogen.

4. Gas permeation tests

We used an experimental setup to evaluate the performance of gas permeation for the prepared membranes as shown in Figure 2. The constant pressure method was considered to measure permeability of the membranes embedded in the membrane module. A counter-current membrane cell, made of stainless steel 316, was utilized to perform the tests. The effective membrane area for permeation was 20 cm^2. The feed gas was transported into the test cell with the outlet valve kept fully closed until the pressure transmitter (PT) specifies the required pressure. The flow rate of the permeate was calculated by bubble flow meter (BFM) after reaching the steady state. The precise composition of the permeate was determined by a gas chromatograph (GC) (ACME 6100, Korea) equipped with a thermal conductivity detector (TCD). In this work, three distinct samples of each studied membrane (synthesized by an exact similar procedure) were tested to measure permeation data. Furthermore, the average of errors is reported within 0.5-3% error margin by using standard deviation analysis. After

each test, the thickness of the membrane was measured using an electronic micrometer (Mitutoyo, No. 293-340, Japan). The thickness of the membranes was 25-40 μm in this work.

The permeability of pure gas was calculated as follows:

$$P = \frac{Q \times l}{A \times \Delta p} \tag{1}$$

where, P is the gas permeability, and Q is the permeate volumetric flow rate (ml s^{-1}); Δp is pressure difference across the membrane (cmHg), and A represents membrane surface area (cm^2); l is membrane thickness (cm). The ratio of the permeability for more permeable gas (A) to that of the less permeable gas (B) is considered as the ideal selectivity of the membrane according to a given pure gas pair as follows:

$$\alpha_{A/B} = \frac{P_A}{P_B} \tag{2}$$

The permeability of the mixed gas can be calculated by:

$$P_A = \frac{Q \times l \times Y_A}{A \times (p_x X_A - p_y Y_A)} \tag{3}$$

where, p_x and p_y stand for the pressures of the feed and permeate respectively; A is the membrane area. The concentration in feed and permeate side are shown by X and Y respectively. The selectivity of the mixed gas for the studied membranes are calculated by:

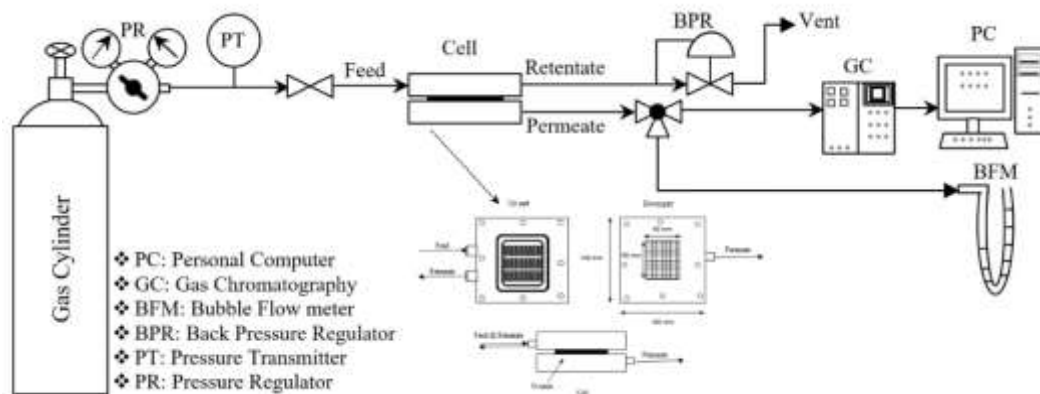$$\alpha_{A/B} = \frac{Y_A/Y_B}{(p_x X_A - p_y Y_A) \Big/ (p_x X_B - p_y Y_B)} \tag{4}$$

Figure 2
A schematic of the designed setup and the module utilized to evaluate the permeation of gases.

5. Results and discussion

5.1. Characterization of NH₂-MIL125

The XRD and FTIR patterns of the prepared NH₂-MIL125 given in Figures 4 and 5 are in good agreement with the results reported in literature (Anjum et al., 2016; Zlotea et al., 2011; Moreira et al.,

2012), and clearly indicate that the as synthesized particles are NH_2-MIL125. The FTIR spectra of NH_2-MIL125 exhibited the characteristics of the stretching vibrations of the hydroxyl at 3461 cm^{-1}, the amino at 3362 cm^{-1}, the carboxylate in the range of 1380-1690 cm^{-1}, and (O-Ti-O) vibrations in the range of 400-769 cm^{-1} (Zhu et al., 2015). The FESEM images of the synthesized NH_2-MIL125 is shown in Figure 6(g), which obviously indicates that the NH_2-MIL125 particles are approximately similar in morphology. CO_2 adsorption analyses were utilized to measure the specific surface area; accordingly, the specific surface area of the synthesized NH_2-MIL125 nanoparticles was 750.23 m^2/g. Furthermore, the results of the particle size distribution of NH_2-MIL125, as illustrated in Figure 3, were determined by the DLS analysis. As can be seen from Figure 3, the particle size of NH_2-MIL125 nanoparticle was within a range of 124.7±4.5 nm. It should be noted that the results of DLS analysis was consistent with the ones obtained by FESEM analysis. These results were in good agreement with the experimental observation reported by other researchers (Vaesen et al., 2013; Anjum et al., 2016).
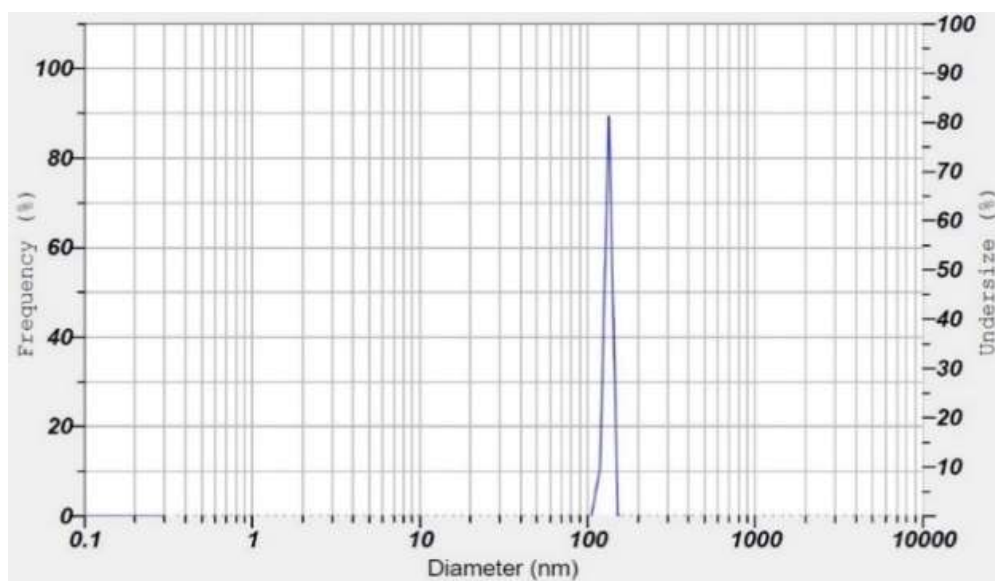

Figure 3
Particle size distribution of NH_2-MIL125.

5.2. Characterization of the prepared membranes

a. X-ray diffraction (XRD)

Figure 4 depicts the XRD patterns of the synthesized pure Pebax, Pebax/PEG(40), Pebax/PEG(40)/NH_2-MIL125(4), Pebax/PEG(40)/NH_2-MIL125(8), Pebax/PEG(40)/NH_2-MIL125(12), and Pebax/PEG(40)/NH_2-MIL125(16) membranes and MOF. A semi-crystalline nature was observed in the neat Pebax membrane with diffraction peaks at 2θ=23.89° and 49.66°. This result was consistent with other similar researches (Murali, Kumar, et al., 2014; Ghasemi Estahbanati et al., 2017). As illustrated in Figure 4, the XRD patterns of the blended membrane show that the intensity and *d*-spacing of the peaks increased, but the position of the peaks decreased by adding PEG 400 into Pebax 1657 matrix. According to the Bragg's equation ($n\lambda=2d\sin\theta$), a reduction in 2θ values increases the *d*-spacing values. *d*-spacing is a measure of the distance between the molecules of the polymer chains. An increase in the value of *d*-spacing states a higher tendency of gas molecules to transport (Zhao et al., 2014; Murali, Ismail, et al., 2014). As shown in Figure 4, the spectra of the composite membranes show peaks of the blended membrane and MOF, which confirms the presence of the blended polymer (Pebax and PEG) and MOF in the prepared composite membranes. Also, increased MOF loading weakens the intensity of the diffraction peak at 2θ= 23.89°. Moreover, an increase in

intersegmental spacing was seen by widening the peak. Embedding the nanoparticle into the blended polymer matrix would decrease its crystallinity, so the membranes became more amorphous (Ghasemi Estahbanati et al., 2017). The change of crystallinity in polymeric membranes definitely affects the gas permeability. Therefore, an enhancement in the permeability of gas is expected because the polymer fractional free volume increases by the addition of the MOF nanoparticles and PEG into the Pebax. This expectation can be fully confirmed by the measurements of gas permeation (Qiu et al., 2016; Hassanajili et al., 2014).

b. Fourier transfer infrared spectroscopy (FTIR)

The FTIR analyses of the neat, blended, and nanocomposite membranes are reported in Figure 5. The neat Pebax has six characteristic peaks at 1111, 1541, 1634, 1733, 2870-2941, and 3302 cm^{-1}. As can be seen, these characteristic peaks are observed in the spectrum of all the membranes, and the characteristic peaks of MOF are seen in the spectrum of the nanocomposite membranes. However, there are slight differences between the neat Pebax and the other membranes. The peak at 1111 cm^{-1} represents the stretching vibration of the ether-oxygen bond C-O-C in the PE segment of Pebax 1657. The comparison between different PEG and MOF loadings showed that this peak widened and shifted to lower wave numbers as the loading increased due to interactions between the ether segment of the polymer, PEG, and nanoparticles (Ghasemi Estahbanati et al., 2017; Merkel et al., 2007). The peaks at 1541 and 1634 cm^{-1} are attributed to amine groups in PA and the bonded and free stretching vibration of C=O group in H-N-C=O in the PE segment (Kim and Lee, 2001; Semsarzadeh et al., 2008). These peaks shift to higher wavenumber up to 10 cm^{-1} after the addition of PEG and MOF nanoparticle. It can also be inferred from this change in the blended and nanocomposite membranes that the nanoparticle and PEG partially disrupted the hydrogen bonding between the PA segment. Therefore, the transport properties of the membranes were enhanced by polar gas. A peak was observed at 1733 cm^{-1} by stretching the vibration of O-C=O group in the PA segment of the polymer. Moreover, C−H functionalities and the N−H bond in the PA phase of the copolymer led to two peaks at 2870−2941 and 3302 cm^{-1} respectively. These obtained results agreed with other related researches (Wang, et al., 2011; Merkel et al., 2007; Sridhar et al., 2007).

c. Field emission scanning electron microscopy (FESEM)

The polymer-nano particle interface quality and the dispersion of MOF particles within the polymer matrix were investigated using FESEM analysis. Figure 6(a-f) displays the images of top surface and cross-sectional membranes. It can be observed that MOF inside the polymer structure has a fully dense structure and is defect-free and well compatible. As illustrated in Figure 6(a and b), two separated microphases are obviously detected in the membranes prepared from pristine Pebax and from Pebax blended with 40 wt.% PEG 400. The PEO segment as the amorphous phase and the crystalline phase (PA) can be represented as oriented polymer lamella (Bondar et al., 1999). By the addition of PEG 400 into Pebax matrix the crystallinity of the membrane decreases because of the removal of intermolecular hydrogen bonds and destroying the lamellar. It implies that the blend membrane has an irregular and convoluted structure. FESEM images, as shown in Figure 6(c-f), show a uniform distribution of MOF particles in the cross-section and top surface of the membrane. The adhesion of NH₂-MIL125 surface with Pebax was considerable because of the hydrogen bonding formation between the amine groups of NH₂-MIL125 and the -OH surface groups of Pebax (Khosravi et al., 2017). However according to Figure 6(c-e), at 4-12 wt.% of NH₂-MIL125, a slight particle agglomeration is observed in top surface of the membrane, while it can be seen in Figure 6(f), at 16 wt.% of NH₂-MIL125, that a large particle agglomeration is observed in the top surface and cross-section of the membrane. As shown in cross-

section images, very thin composite membranes are obtained, so the transport mechanism could be considered solution–diffusion.
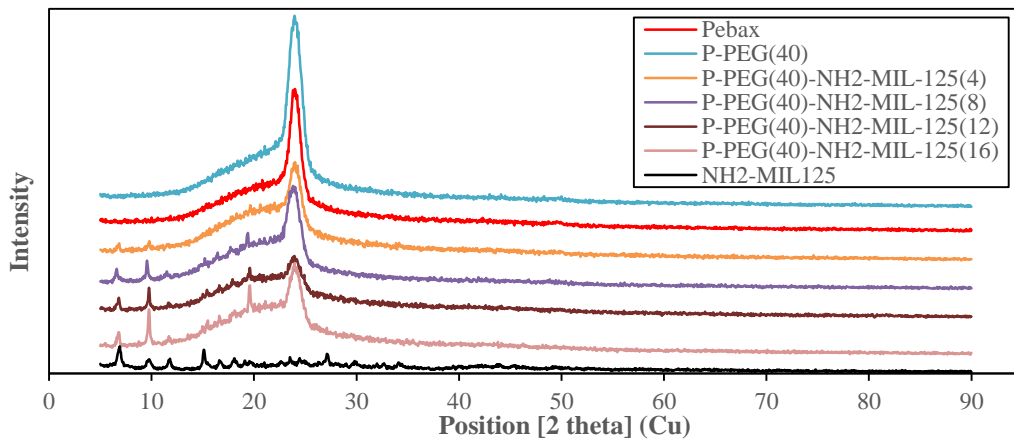

Figure 4

The XRD patterns of the synthesized NH_2-MIL125 and pure Pebax, Pebax/PEG(40), Pebax/PEG(40)/NH_2-MIL125(4), Pebax/PEG(40)/NH_2-MIL125(8), Pebax/PEG(40)/NH_2-MIL125(12), and Pebax/PEG(40)/NH_2-MIL125(16) membranes.
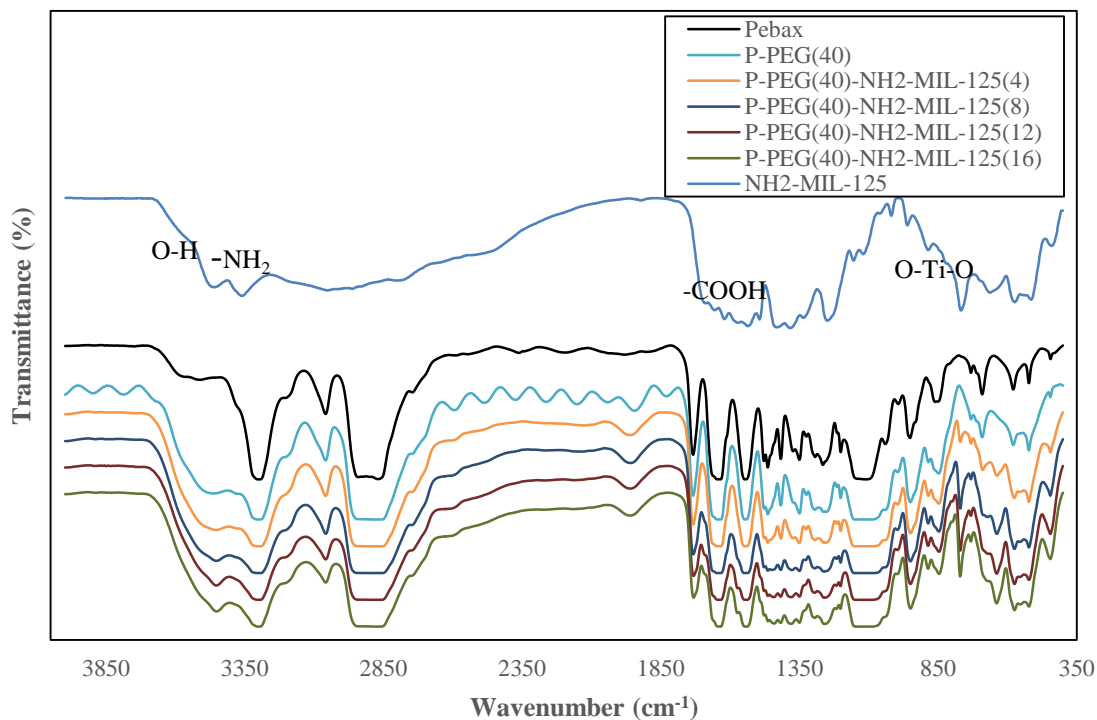

Figure 5

FTIR spectra of the synthesized NH_2-MIL125 and pure Pebax, Pebax/PEG(40), Pebax/PEG(40)/NH_2-MIL125(4), Pebax/PEG(40)/NH_2-MIL125(8), Pebax/PEG(40)/NH_2-MIL125(12), and Pebax/PEG(40)/NH_2-MIL125(16) membranes.
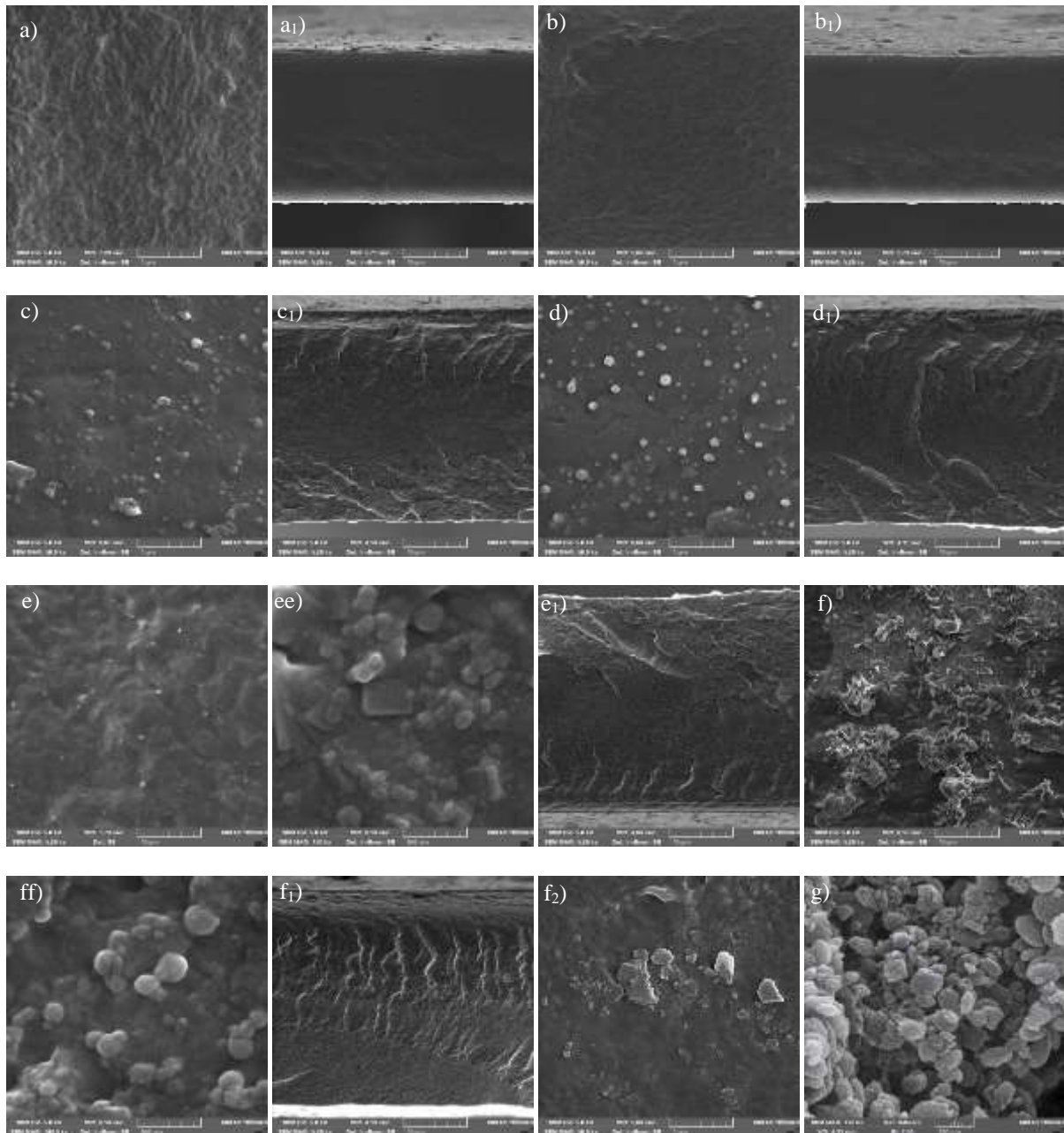
Figure 6

FESEM images of membranes: a) pure Pebax, b) Pebax/PEG(40), c) Pebax/PEG(40)/NH$_2$-MIL125(4), d) Pebax/PEG(40)/NH$_2$-MIL125(8), e) Pebax/PEG(40)/NH$_2$-MIL125(12), f) Pebax/PEG(40)/NH$_2$-MIL125(16) top surface (letter) and cross-section (letter with a subscript), and g) NH$_2$-MIL125.

5.3. Gas permeation measurements

First, the effects of PEG 400 addition to the Pebax 1657 matrix on their transport features were evaluated with the gas permeation behavior of the pure and mixed gases through the blended membranes having 10, 20, 30, and 40 wt.% Pebax PEG 400. Afterwards, the best membrane was selected for modification by NH$_2$-MIL125 nanoparticles. The Pebax/PEG/NH$_2$-MIL125 nanocomposite membranes containing various amounts of NH$_2$-MIL125 (4, 8, 12, and 16 wt.% of polymeric blend (Pebax & PEG)) were investigated in the same way. All the experimental data are obtained at a constant feed pressure of 2 bar and ambient temperature (about 24-26 °C). Finally, the separation performance (pure and mixed

gases) of the pristine Pebax, blended, and nanocomposite membranes with the optimum amount of PEG 400 and NH_2-MIL125 nanoparticles was compared at different feed pressures (2, 4, 6, and 8 bar) and ambient temperature.

a. Pure gas permeation performances

Effect of PEG

Figure 7(a and b) shows the pure gas permeabilities and ideal CO_2/CH_4 selectivities of the blended membranes as a function of the PEG 400 loading. As can be seen from Figure 7(a), the permeabilities of pure gases (CO_2 and CH_4) are increased by adding PEG 400 into the Pebax matrix, but this increase for CO_2 is more than that for CH_4. The PEG 400 is naturally amorphous, so the increase in CO_2 permeability in the blended membranes can be attributed to the increased decrystallization of both PEO and PA segments in the Pebax matrix. Therefore, the amount of amorphous EO segments and consequently fractional free-volume of the membranes are increased. In other words, the affinity between CO_2 and the polymer matrix is enhanced with the addition of the polar ether groups of PEG 400, so the solubility and selectivity of blended membranes are increased (Reijerkerk et al., 2010; Car et al., 2008b; Azizi et al., 2017b; Azizi et al., 2017). The solubility and permeability of CO_2 are increased by increasing PEG 400 loading more than those of CH_4. It is expected that PEG 400 as an additive in the Pebax increases the ideal CO_2/CH_4 selectivity as shown in Figure 7(b). Therefore, the prepared blended membranes had better performance for CO_2 separation from CH_4 in comparison with the pristine Pebax 1657 membrane. The performance of the blended membrane containing 40 wt.% PEG 400 was the best among the other blends. The permeabilities of pure gases of CO_2 and CH_4, and the ideal CO_2/CH_4 selectivity are respectively increased from 84.6 and 4.71 Barrer and 17.96 for pristine Pebax 1657 to 160.76 and 8.39 Barrer and 19.16 for the blended membrane having 40 wt.% PEG 400 as an additive.
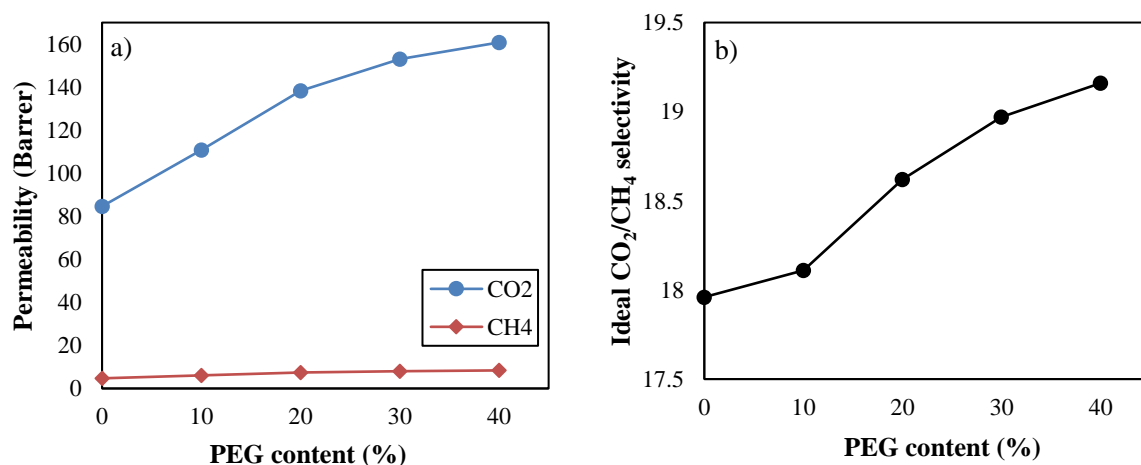

Figure 7
Effect of PEG 400 on gas permeation performance of the prepared membranes at 2 bar; a) CO_2 and CH_4 permeability and b) ideal CO_2/CH_4 selectivity.

Effect of NH_2-MIL125 nanoparticles

Figure 8(a-c) shows the effects of the NH_2-MIL125 loading on gas separation and permeation of Pebax/PEG membranes having 40 wt.% PEG 400 compared to the pristine and selected blended Pebax/PEG membranes at a feed pressure of 2 bar and ambient temperature. All the nanocomposite membranes showed a high improvement in CO_2 permeability and ideal CO_2/CH_4 selectivity relative to

the pristine Pebax and reference membranes, while CH_4 permeabilities showed a slightly decreasing behavior. This enhancement in CO_2 permeability without a decrease in selectivity implies that the most of gas passes through the porous structure of the NH_2-MIL125 nanoparticles, leading to this conclusion that the membranes are really defect-free (Anjum et al., 2016) as also shown in FESEM pictures. Small micropores in the nanoparticles allow the penetrated gas molecules to react with the -OH and -NH_2 groups in the nanoparticles, so selectivity is increased in these membranes (Kim et al., 2013). In general, the increase in the selectivity of the nanocomposite membranes, compared to the unfilled membranes, can be explained by the presence of the amine groups in the nanoparticles. These groups form additional CO_2 selective sites and provide good hydrogen bonding with CO_2. Therefore, the affinity with the CH_4 molecules is reduced, and they can pass through the nanocomposite membranes (Kim et al., 2013). In addition, the separation performance of the nanocomposite membranes is enhanced due to the high interactions of the nanoparticles with the polymeric matrix. Likewise, covalent bonds are established among the -NH_2 groups at the nanoparticle surface and those on polymer chains (Guo et al., 2015; Anjum et al., 2016). These effects do not counteract with the smaller surface area of NH_2-MIL125 (Zheng et al., 2010). As shown in Figure 8(c), the ideal CO_2/CH_4 selectivity for 16 wt.% nanoparticle loading is decreased by decreasing the CO_2 permeability and increasing the CH_4 permeability. This can be explained by the formation of interfacial voids between filler and polymer because filler dispersion may be eventually worsened at higher loadings (Basu et al., 2011). As previously described and shown in Figure 6, this behavior may be owing to the fact that nanoparticles bond together and form agglomeration; as a result, the number of nanoparticles entering into the membrane polymer network decreases, so the CO_2 selective sites in the nanocomposite membrane are reduced.
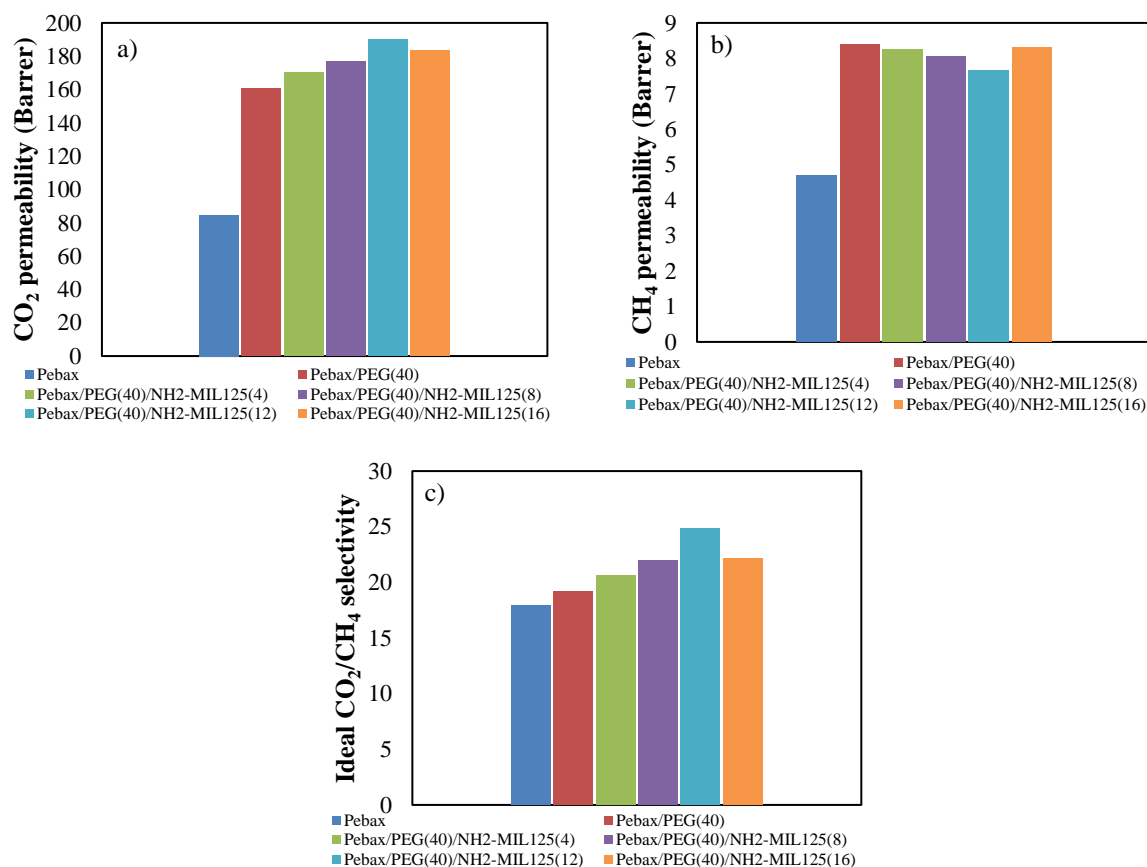

Figure 8

Effect of NH_2-MIL125 on gas permeation performance of the prepared membranes at 2 bar; a) CO_2 permeability, b) CH_4 permeability, and c) ideal CO_2/CH_4 selectivity.

Effect of feed pressure

The effect of feed pressure on the permeability and selectivity performance of the membrane is investigated in the case of the blended Pebax/PEG 400 with 40 wt.% PEG 400 loading, the nanocomposite Pebax/PEG/NH_2-MIL125 with 12 wt.% NH_2-MIL125 (as they had the best performance), and the pristine Pebax. The performance of the mentioned membranes was evaluated for the pure and mixed (10 vol.% CO_2, 90 vol.% CH_4) gases at ambient temperature and in a feed pressure range of 2-8 bar.

As illustrated in Figures 9(a-c) and Figure 11(a-c), the CO_2/CH_4 selectivities and permeabilities of CO_2 and CH_4 for the pure and mixed gases in all the membranes are increased. This increase in CO_2 permeabilities, compared to CH_4, was more significant. The competition between plasticization and compaction affects the permeability of polar gases (such as CO_2) (Feng et al., 2013). The absorption of CO_2 increased by increasing the pressure since the membrane was more plasticized (increased chain flexibility) and a higher fractional free volume and consequently permeability was obtained (Khosravi et al., 2017). CO_2 had a smaller kinetic diameter (3.3 Å) than CH_4 (3.8 Å), and it was a condensable gas with a higher affinity for polar groups in polymer matrix; thus, it could show higher permeabilities through the membranes (Wang et al., 2014). In other words, Pebax having PEO is a stronger absorber for CO_2, so the solubility of CO_2 in this polymer is considerably high. Also, the solubility of CO_2 in all the membranes was increased at a higher pressure of the feed. Consequently, the permeability of CO_2 in all the membranes increased by raising pressure because the permeability of CO_2 in these membranes is mainly affected by its solubility rather than its diffusivity (Jomekian et al., 2017). As shown in Figures 9 and 11(a and b), the increasing trend in both CH_4 and CO_2 permeabilities through the blend Pebax/PEG(400) membrane decreases by raising pressure. The reason for this behavior can be attributed to the fact that the blend membrane had a higher free volume, so increased pressure caused a reduction in free volume and chain flexibility, which led to a relative lower increase in permeability as a function of pressure (Reijerkerk et al., 2010).

The permeability of CO_2 through the composite membrane, compared to the other membranes, is more intensive; in fact, because of the presence of numerous active polar -NH_2 sites in the membrane, the tendency for sorption and the solubility of CO_2 in this membrane are strongly increased. Furthermore, the porosity and micron-sized holes in nanoparticles, existed in the membrane, can act as a factor increasing the permeation of CO_2 and CH_4 in the nanocomposite membrane for the pure and mixed gases. According to the data obtained at increased pressure, the CO_2 permeability through all the membranes, for the pure and mixed gases, was higher compared to methane permeability. It is anticipated that ideal and real CO_2/CH_4 selectivity would also be increased by increasing pressure, but the increase for the case of mixed gases was lower as well illustrated in Figure 10. To draw analogy between the behaviors of membrane under the pressure, carbon dioxide/methane permeabilities and ideal and real carbon dioxide/methane selectivity values are presented in Table 1.
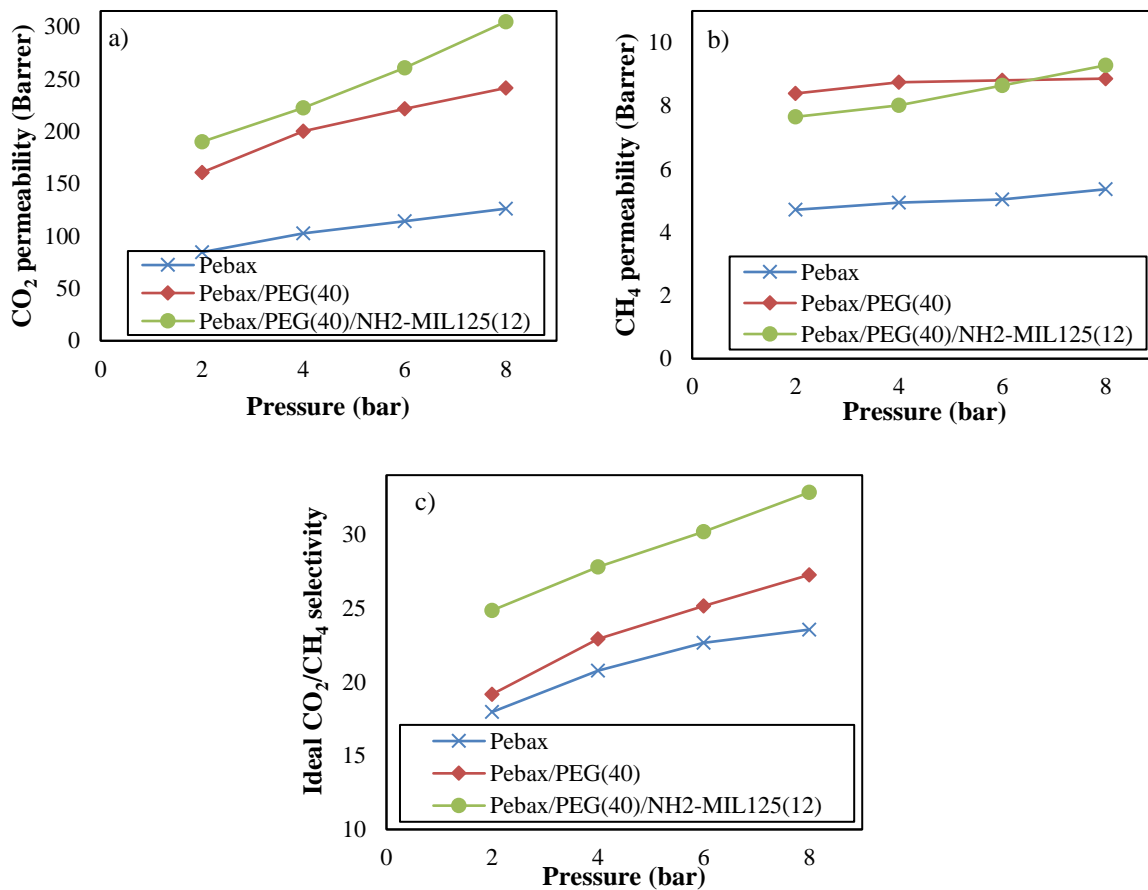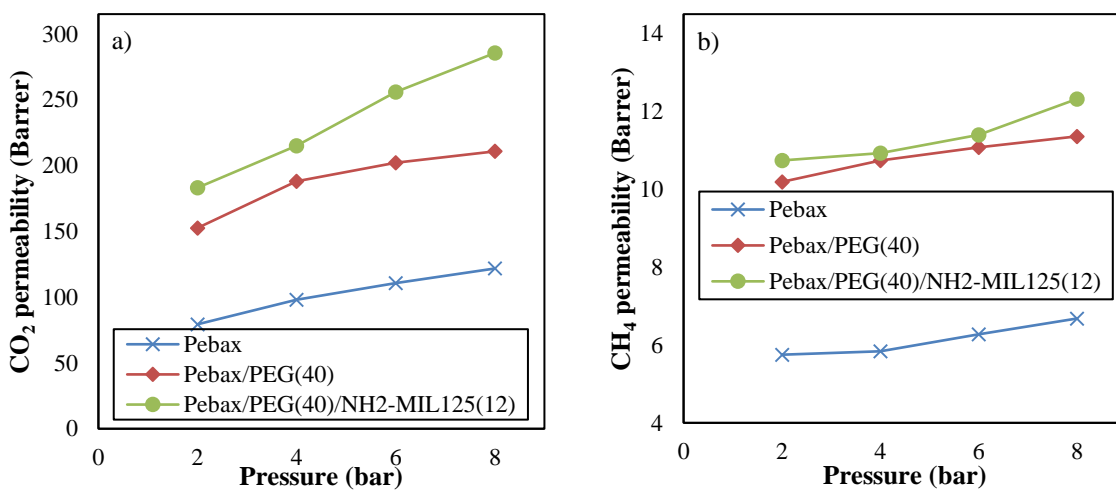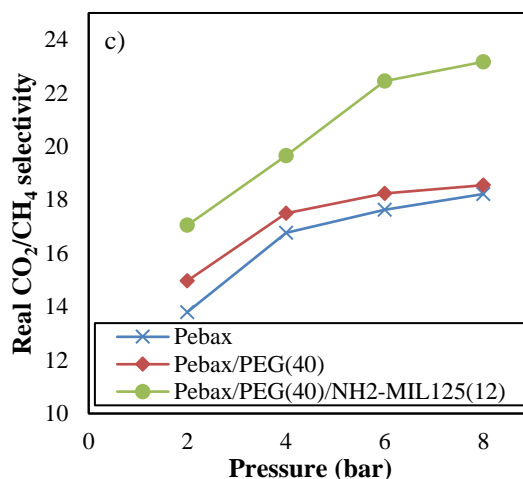
Figure 9

Effect of pressure on gas permeation performance of pristine Pebax, Pebax/PEG(40), and Pebax/PEG(40)/NH$_2$-MIL125(12) membranes at 2-8 bar; a) CO$_2$ permeability, b) CH$_4$ permeability, and c) ideal CO$_2$/CH$_4$ selectivity.

Figure 10

Effect of pressure on gas permeation performance of pristine Pebax, Pebax/PEG(40), and Pebax/PEG(40)/NH$_2$-MIL125(12) membranes at 2-8 bar; a) CO$_2$ permeability, b) CH$_4$ permeability, and c) real CO$_2$/CH$_4$ selectivity.

Table 1

The CO$_2$ and CH$_4$ permeabilities (in Barrer), ideal and real CO$_2$/CH$_4$ selectivities of Pebax, Pebax/PEG(40), and Pebax/PEG(40)/NH$_2$-MIL125(12) at different feed pressures obtained in the pure and mixed gases tests.

Membrane	Parameter	Gas	Feed pressure (bar)							
			2		4		6		8	
			Pure	Mix	Pure	Mix	Pure	Mix	Pure	Mix
Pebax	Permeability	CO$_2$	84.60	79.35	102.56	97.95	114.16	110.55	126.18	121.74
	Permeability	CH$_4$	4.71	5.75	4.94	5.84	5.04	6.27	5.36	6.68
	Selectivity	CO$_2$/CH$_4$	17.96	13.80	20.76	16.77	22.65	17.63	23.54	18.22
Pebax/PEG(40)	Permeability	CO$_2$	160.76	152.54	200.15	187.95	221.51	202.12	241.44	210.73
	Permeability	CH$_4$	8.39	10.19	8.74	10.74	8.81	11.08	8.86	11.36
	Selectivity	CO$_2$/CH$_4$	19.16	14.97	22.90	17.50	25.14	18.24	27.25	18.55
Pebax/PEG(40)/ NH$_2$- MIL125(12)	Permeability	CO$_2$	190.03	183.11	222.52	214.88	260.67	255.93	304.76	285.45
	Permeability	CH$_4$	7.65	10.74	8.01	10.93	8.64	11.40	9.28	12.32
	Selectivity	CO$_2$/CH$_4$	24.84	17.05	27.78	19.66	30.17	22.45	32.84	23.17

b. Mixed gas permeation performances

Mixed gas experiments were performed with 90 vol.% CH$_4$ and 10 vol.% CO$_2$ in the feed at ambient temperature and at a feed pressure of 2 bar; the results are shown in Table 2 and Figures 11(a-d) and 12(a-c). As can be seen, the same changes in permeability and selectivity are observed for both pure and mixed gases. However, in the same conditions, the permeability of CO$_2$, in comparison with the pure gas, reduced, while that of and CH$_4$ increased; also, the real CO$_2$/CH$_4$ selectivity is reduced. This behavior can be interpreted by the plasticization of PEO groups in the polymer matrix.

The -NH$_2$ and -OH groups in the nanoparticles and PEO groups in polymer matrix had a high affinity for CO$_2$, so the excessive absorption of CO$_2$ results in the plasticization of the membranes. This changes the inherent separation properties of the membranes. As a result, the permeability of CH$_4$ is greater for the case of mixed gases compared to the single gas tests. Generally, higher absorption of the permeant in the polymer causes the swelling of the membrane material (Liu et al., 2005).
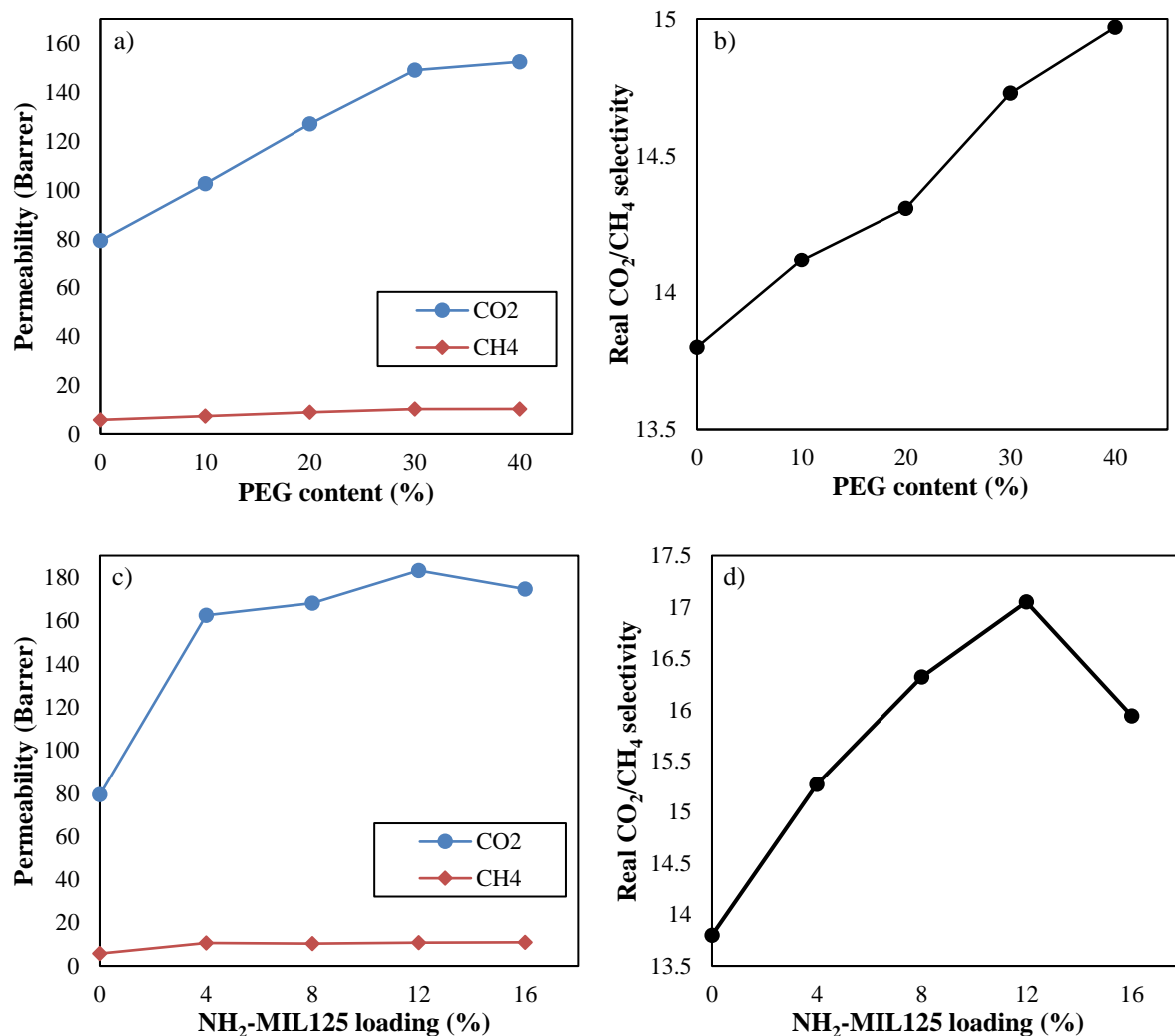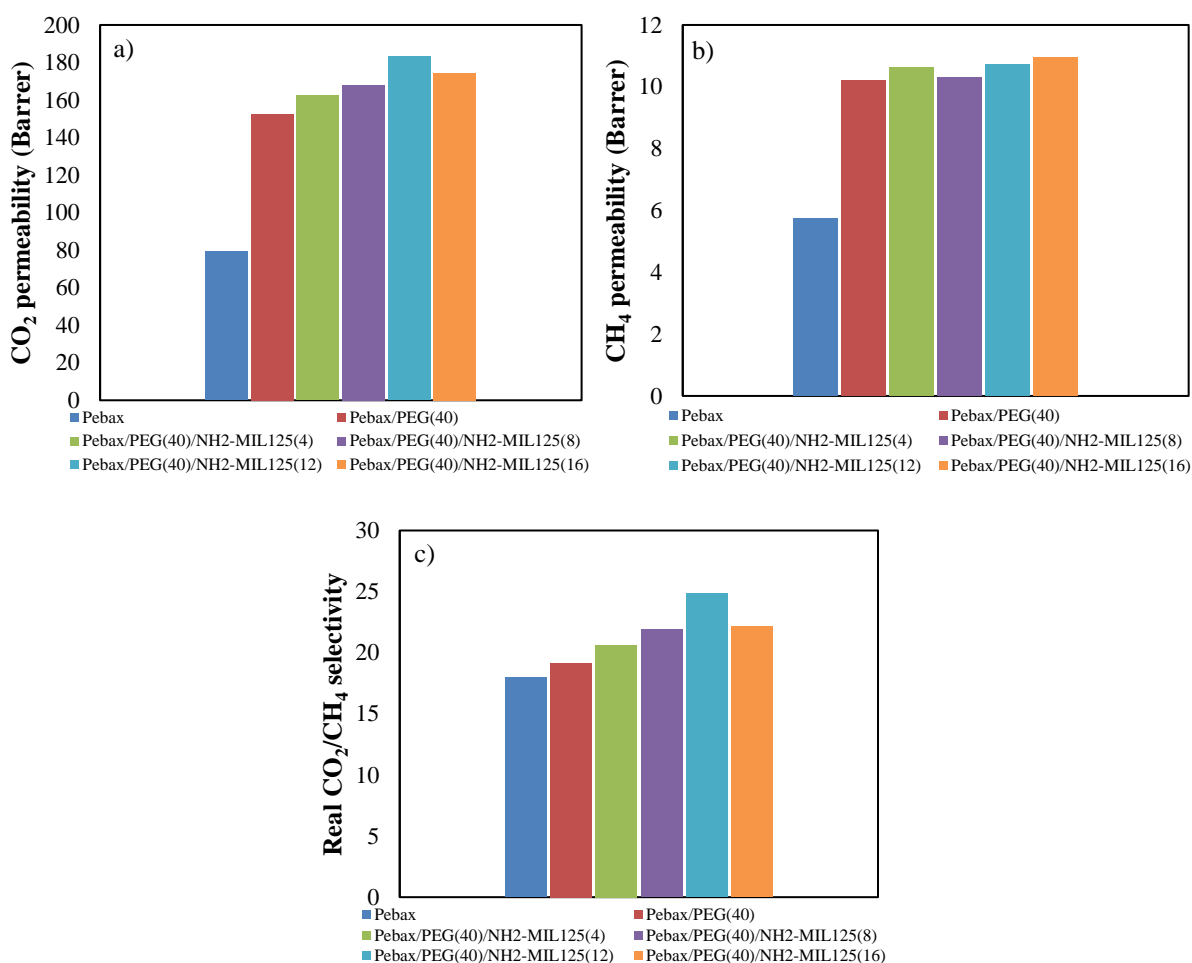

Figure 11
Effect of PEG 400 on mix gas permeation performance of the prepared membranes at 2 bar; a) and c) CO$_2$ and CH$_4$ permeability and b) and d) real CO$_2$/CH$_4$ selectivity.

Figure 12

Effect of NH_2-MIL125 on mix gas permeation performance of the prepared membranes at 2 bar; a) CO_2 permeability, b) CH_4 permeability, and c) real CO_2/CH_4 selectivity.

Table 2

The CO_2 and CH_4 permeabilities and real CO_2/CH_4 selectivities of the prepared membranes at a feed pressure of 2 bar obtained in the mixed gases tests.

Membrane	CO_2 permeability (Barrer)		CH_4 permeability (Barrer)		CO_2/CH_4 selectivity	
	Pure	Mix	Pure	Mix	Pure	Mix
Pebax	84.60	79.35	4.71	5.75	17.96	13.80
Pebax/PEG(10)	110.83	102.65	6.12	7.27	18.11	14.12
Pebax/PEG(20)	138.35	127.07	7.43	8.88	18.62	14.31
Pebax/PEG(30)	153.05	149.07	8.07	10.12	18.97	14.73
Pebax/PEG(40)	160.76	152.54	8.39	10.19	19.16	14.97
Pebax/PEG(40)/NH_2-MIL125(4)	170.07	162.47	8.24	10.64	20.64	15.27
Pebax/PEG(40)/NH_2-MIL125(8)	176.75	168.10	8.06	10.30	21.93	16.32
Pebax/PEG(40)/NH_2-MIL125(12)	190.03	183.11	7.65	10.74	24.84	17.05
Pebax/PEG(40)/NH_2-MIL125(16)	183.60	174.54	8.30	10.95	22.12	15.94

6. Conclusions

In the current work, PEG 400 and NH_2-MIL125 nanoparticles were added to the Pebax 1657 network to produce polymer nanocomposite membranes in order to improve CO_2/CH_4 gas separation performance. The results showed that the Pebax/PEG 400 blend membranes are superior to the pristine Pebax membrane, in the same conditions, and Pebax/PEG 400/NH_2-MIL125 nanocomposite membranes are better than the polymer blend membranes. This increase in separation performance is due to the reduction in crystallinity, which leads in turn to an augmented free volume in the polymer matrix. Also, the $-NH_2$ and -OH groups in the nanoparticles and PEO groups in polymer matrix had a high affinity for CO_2, so the excessive absorption of CO_2 resulted in the plasticization of the membranes. In addition, the micro pores in the nanoparticles allowed a significant part of the gas to pass through the membrane. The highest values of CO_2 permeation and ideal CO_2/CH_4 selectivity were observed in the polymer nanocomposite membrane with 40 wt.% PEG 400 and 12 wt.% NH_2-MIL125. The highest ideal selectivity of CO_2/CH_4 and CO_2 permeability at a pressure of 8 bar and ambient temperature were increased to 32.84 and 304.76 Barrer respectively. In addition, the real selectivity of CO_2/CH_4 and CO_2 permeability, in a condition similar to that of mixed gases tests, increased to 23.17 and 285.45 Barrer respectively. The mixed gas permeability results indicated that the fabricated polymer nanocomposite membrane had the best performance in separating CO_2 from the gas mixture and can be considered as a reliable alternative in gas separation processes such as sweetening sour gas.

Acknowledgements

References

Adewole, J. K., Ahmad, A. L., Sultan, A. S., Ismail, S., and Leo, C. P., Model-based Analysis of Polymeric Membranes Performance in High Pressure CO_2 Removal from Natural Gas, Journal of Polymer Research, Vol. 22, No. 3, p. 32, 2015.

Anjum, M. W., Bueken, B., Vos, D. D., and Vankelecom, F. J., MIL-125 (Ti) Based Mixed Matrix Membranes for CO_2 Separation from CH_4 and N_2, Journal of Membrane Science, Vol. 502, p. 21-28, 2016.

Asadi, T., and Ehsani, M., An Experimental Study of Adsorption Breakthrough Curves for CO_2/CH_4 Separation in a Fixed Bed of Nanoporous Shaped Copper Trimesate Metal Organic Framework, Iranian Journal of Oil & Gas Science and Technology, Vol. 2, No. 4, p. 54-66, 2013.

Azizi, N., Mahdavi, H. R., Isanejad, M., and Mohammadi, T., Effects of Low and High Molecular Mass PEG Incorporation into Different Types of Poly (Ether-b-Amide) Copolymers on the Permeation Properties of CO_2 and CH_4, Journal of Polymer Research, Vol. 24, No. 9, p. 141, 2017.

Azizi, N., Mohammadi, T., and Behbahani, R. M., Synthesis of a New Nanocomposite Membrane (PEBAX-1074/PEG-400/TiO_2) in Order to Separate CO_2 from CH_4, Journal of Natural Gas Science and Engineering, Vol. 37, p. 39-51, 2017.

Azizi, N., Mohammadi,T., and Behbahani, R. M., Synthesis of a PEBAX-1074/ZnO Nanocomposite Membrane with Improved CO_2 Separation Performance, Journal of Energy Chemistry, Vol. 26, No. 3, p. 454-465, 2017.

Baker, R. W., Future Directions of Membrane Gas Separation Technology, Industrial & Engineering Chemistry Research, Vol. 41, No. 6, p. 1393-1411, 2002.

Basu, S., Cano-Odena A., and Vankelecom, F. J., MOF-containing Mixed-matrix Membranes for CO_2/CH_4 and CO_2/N_2 Binary Gas Mixture Separations, Separation and Purification Technology, Vol. 81, No. 1, p. 31-40, 2011.

Bondar, V. I., Freeman, B. D., and Pinnau, I., Gas Sorption and Characterization of Poly (Ether- b- Amide) Segmented Block Copolymers, Journal of Polymer Science Part B: Polymer Physics, Vol. 37, No. 17, p. 2463-2475, 1999.

Car, A., Stropnik, C., Yave, W., and Peinemann, K., PEG Modified Poly (Amide-b-Ethylene Oxide) Membranes for CO_2 Separation, Journal of Membrane Science, Vol. 307, No. 1, p. 88-95, 2008.

Car, A., Stropnik, C., Yave, W., and Peinemann, K., Pebax®/Polyethylene Glycol Blend Thin Film Composite Membranes for CO_2 Separation: Performance with Mixed Gases, Separation and Purification Technology, Vol. 62, No. 1, p. 110-117, 2008.

Cho, E. H., Kim, K. B., and Rhim, J. W., Transport Properties of PEBAX Blended Membranes with PEG and Glutaraldehyde for SO_2 and Other Gases, Polymer Korea, Vol. 38, No. 6, p. 687-693, 2014.

Cong, H., Yu, B., Tang, J., and Zhao, X. S., Ionic Liquid Modified Poly (2, 6-Dimethyl-1, 4-Phenylene Oxide) for CO_2 Separation, Journal of Polymer Research, Vol. 19, No. 2, p. 9761, 2012.

Dan-Hardi, M., Serre, C., Frot, T., Rozes, L., Maurin, G., Sanchez, C., and Férey, G., A New Photoactive Crystalline Highly Porous Titanium (IV) Dicarboxylate, Journal of the American Chemical Society, Vol. 131, No. 31, p. 10857-10859, 2009.

Diestel, L., Wang, N., Schulz, A., Steinbach, F., and Caro, J., Matrimid-based Mixed Matrix Membranes: Interpretation and Correlation of Experimental Findings for Zeolitic Imidazolate Frameworks as Fillers in H_2/CO_2 Separation, Industrial & Engineering Chemistry Research, Vol. 54, No. 3, p. 1103-1112, 2015.

Feng, S., Ren, J., Hua, K., Li, H., Ren, X., and Deng, M., Poly (Amide-12-b-Ethylene Oxide)/Polyethylene Glycol Blend Membranes for Carbon Dioxide Separation, Separation and Purification Technology, Vol. 116, p. 25-34, 2013

Flesher, J. R., Pebax® Polyether Block Amide-a New Family of Engineering Thermoplastic Elastomers, in, High Performance Polymers: Their Origin and Development, 401-408 p., Springer Publication., 1986.

Frot, T., Cochet, S., Laurent, G., Sassoye, C., Popall, M., Sanchez, C., and Rozes, L., Ti_8O_8 (OOCR) 16, a New Family of Titanium–oxo Clusters: Potential NBUs for Reticular Chemistry, European Journal of Inorganic Chemistry, Vol. 2010, No. 36, p. 5650-5659, 2010.

Fu, Y., Sun, D., Chen, Y., Huang, R., Ding, Z., Fu, X., and Li, Z., An Amine- functionalized Titanium Metal–organic Framework Photocatalyst with Visible- Light- Induced Activity for CO_2 Reduction, Angewandte Chemie International Edition, Vol. 51, No. 14, p. 3364-3367, 2012.

Ghaemi, A., Hashemzadeh V., and Shahhosseini, Sh., An Experimental Investigation of Reactive Absorption of Carbon Dioxide into an Aqueous $NH_3/H_2O/NaOH$ Solution, Iranian Journal of Oil & Gas Science and Technology, Vol. 6, No. 3, p. 55-67, 2017.

Ghasemi E. E., Omidkhah, M., and Amooghin, A. E., Interfacial Design of Ternary Mixed Matrix Membranes Containing Pebax1657/Silver-Nanopowder/[BMIM][BF$_4$] for Improved CO_2 Separation Performance, ACS Applied Materials & Interfaces, Vol. 9, No. 11, p. 10094-10105, 2017.

Guo, X., Huang, H., Ban, Y., Yang, Q., Xiao, Y., Li, Y., Yang, W., and Zhong, C., Mixed Matrix Membranes Incorporated with Amine-functionalized Titanium-based Metal-organic Framework for CO_2/CH_4 Separation, Journal of Membrane Science, Vol. 478, p. 130-139, 2015.

Habibzare, S., Asghari, M., and Djirsarai, A., Nano Composite PEBAX®/PEG Membranes: Effect of MWNT Filler on CO_2/CH_4 Separation, International Journal of Nano Dimension, Vol. 5, p. 247-254, 2014.

Hassanajili, S., Khademi, M. A., and Keshavarz, P., Influence of Various Types of Silica Nanoparticles on Permeation Properties of Polyurethane/Silica Mixed Matrix Membranes, Journal of Membrane Science, Vol. 453, p. 369-383, 2014.

Jomekian, A., Behbahani, R. M., Mohammadi, T., and Kargari, A., High Speed Spin Coating in Fabrication of Pebax 1657 Based Mixed Matrix Membrane Filled with Ultra-porous ZIF-8 Particles for CO_2/CH_4 Separation, Korean Journal of Chemical Engineering, Vol. 34, No. 2, p. 440-453, 2017.

Khosravi, T., Omidkhah, M. R., Kaliaguine, S., and Rodrigue, D., Amine- functionalized CuBTC/Poly (Ether- b- Amide- 6)(Pebax® MH 1657) Mixed Matrix Membranes for CO_2/CH_4 Separation, The Canadian Journal of Chemical Engineering, Vol. 95, No. 10, p. 2024-2033, 2017.

Kim, J. H., and Lee, Y. M., Gas Permeation Properties of Poly (Amide-6-b-Ethylene Oxide)–Silica Hybrid Membranes, Journal of Membrane Science, Vol. 193, No. 2, p. 209-225, 2001.

Kim, S., Kim, J., Kim, H. Y., Cho, H., and Ahn, W., Adsorption/Catalytic Properties of MIL-125 and NH$_2$-MIL-125, Catalysis Today, Vol. 204, p. 85-93, 2013.

Li, T., Pan, Y., Peinemann, K. V., and Lai, Z., Carbon Dioxide Selective Mixed Matrix Composite Membrane Containing ZIF-7 Nano-fillers, Journal of Membrane Science, Vol. 425, p. 235-242, 2013.

Li, Y., and Chung, T. S., Molecular-level Mixed Matrix Membranes Comprising Pebax® and POSS for Hydrogen Purification via Preferential CO_2 Removal, International Journal of Hydrogen Energy, Vol. 35, No. 19, p. 10560-10568, 2010.

Lin, H., and Freeman, B. D., Materials Selection Guidelines for Membranes that Remove CO_2 from Gas Mixtures, Journal of Molecular Structure, Vol. 739, No. 1-3 , p. 57-74, 2005.

Liu, H., Zhao, Y., Zhang, Z., Nijem, N., Chabal, Y. J., Peng, X., Zeng, H., and Li, J., Ligand Functionalization and its Effect on CO_2 Adsorption in Microporous Metal–organic Frameworks, Chemistry–An Asian Journal, Vol. 8, No. 4, p. 778-785, 2013.

Liu, L., Chakma, A., and Feng, X., CO_2/N_2 Separation by Poly (Ether Block Amide) Thin Film Hollow Fiber Composite Membranes, Industrial & Engineering Chemistry Research, Vol. 44, No. 17, p. 6874-6882, 2005.

Mahmoudi, A., Asghari, M., and Zargar, V., CO_2/CH_4 Separation Through a Novel Commercializable Three-phase PEBA/PEG/NaX Nanocomposite Membrane, Journal of Industrial and Engineering Chemistry, Vol. 23, p. 238-242, 2015.

Merkel, T. C., Blanc, R., Zeid, J., Suwarlim, A., Firat, B., Wijmans, H., Asaro, M., and Greene, M. L., Separation of Olefin/Paraffin Mixtures with Carrier Facilitated Membrane Final Report, Membrane Technology and Research, Inc., Menlo Park, CA. 2007.

Moreira, M. A., Santos, J. C., Ferreira, A. F. P., Loureiro, J. M., Ragon, F., Horcajada, P., Yot, P. G., Serre, C., and Rodrigues, E. A., Effect of Ethylbenzene in P-xylene Selectivity of the Porous Titanium Amino Terephthalate MIL-125(Ti) _NH$_2$, Microporous and Mesoporous Materials, Vol. 158, p. 229-234, 2012.

Murali, R. S., Ismail, A. F., Rahman, Mukhlis, A., and Sridhar, S., Mixed Matrix Membranes of Pebax-1657 Loaded with 4A Zeolite for Gaseous Separations, Vol. 129, p. 1-8, 2014.

Murali, R. S., Kumar, K. P., Ismail, A. F., and Sridhar, S., Nanosilica and H-Mordenite Incorporated Poly (Ether-Block-Amide)-1657 Membranes for Gaseous Separations, Microporous and Mesoporous Materials, Vol. 197, p. 291-298, 2014.

Naseri, M., Mousavi, S. F., Mohammadi, T., and Bakhtiari, O., Synthesis and Gas Transport Performance of MIL-101/Matrimid Mixed Matrix Membranes, Journal of Industrial and Engineering Chemistry, Vol. 29, p. 249-256, 2015.

Qiu, Y., Ren, J., Zhao, D., Li, H., and Deng, M., Poly (Amide-6-b-Ethylene Oxide)/[Bmim][Tf$_2$N] Blend Membranes for Carbon Dioxide Separation, Journal of Energy Chemistry, Vol. 25, No. 1, p. 122-130, 2016.

Reijerkerk, S. R., Knoef, M. H., Nijmeijer, K., and Wessling, M., Poly (Ethylene Glycol) and Poly (Dimethyl Siloxane): Combining their Advantages into Efficient CO$_2$ Gas Separation Membranes, Journal of Membrane Science, Vol. 352, No. 1-2, p. 126-135, 2010.

Robeson, L. M., Correlation of Separation Factor Versus Permeability for Polymeric Membranes, Journal of Membrane Science, Vol. 62, No. 2, p. 165-185, 1991.

Semsarzadeh, M. A., Sadeghi, M., and Barikani, M., Effect of Chain Extender Length on Gas Permeation Properties of Polyurethane Membranes, Iranian Polymer Journal, Vol. 17, No. 6, p. 431-440, 2008.

Sridhar, S., Aminabhavi, T. M., Mayor, S. J., and Ramakrishna, M., Permeation of Carbon Dioxide and Methane Gases Through Novel Silver-incorporated Thin Film Composite Pebax Membranes, Industrial & Engineering Chemistry Research, Vol. 46, No. 24, p. 8144-8151, 2007

Vaesen, S., Guillerm, V., Yang, Q., Wiersum, A. D., Marszalek, B., Gil, B., Vimont, A., Daturi, M., Devic, T., and Llewellyn, P. L., A Robust Amino-functionalized Titanium (IV) Based MOF for Improved Separation of Acid Gases, Chemical Communications, Vol. 48, No. 86, p. 10082-10084, 2013.

Wang, S., Liu, Y., Huang, S., Wu, H., Li, Y., Tian, Z., and Jiang, Z., Pebax–PEG–MWCNT Hybrid Membranes with Enhanced CO$_2$ Capture Properties, Journal of Membrane Science, Vol. 460, p. 62-70, 2014.

Wang, Y., Ren, J., and Deng, M., Ultrathin Solid Polymer Electrolyte PEI/Pebax2533/AgBF$_4$ Composite Membrane for Propylene/Propane Separation, Separation and Purification Technology, Vol. 77, No. 1, p. 46-52, 2011.

Yang, Z. Z., Song, Q. W., and He, L. N., Capture and Utilization of Carbon Dioxide with Polyethylene Glycol, Springer Science & Business Media Publication, 2012

Zhao, D., Ren, J., Li, H., Li, X., and Deng, M., Gas Separation Properties of Poly (Amide-6-b-Ethylene Oxide)/Amino Modified Multi-walled Carbon Nanotubes Mixed Matrix Membranes, Journal of Membrane Science, Vol. 467, p. 41-47, 2014.

Zheng, B., Bai, J., Duan, J., Wojtas, L., and Zaworotko, M., Enhanced CO$_2$ Binding Affinity of a High-uptake rht-Type Metal−organic Framework Decorated with Acylamide Groups, Journal of the American Chemical Society, Vol. 133, No. 4, p. 748-751, 2010.

Zhu, W., Liu, P., Xiao, S., Wang, W., Zhang, D., and Li. H., Microwave-assisted Synthesis of Ag-doped MOFs-like Organotitanium Polymer with High Activity in Visible-light Driven Photocatalytic NO Oxidization, Applied Catalysis B: Environmental, Vol. 172, p. 46-51, 2015.

Zlotea, C., Phanon, D., Mazaj, M., Heurtaux, D., Guillerm, V., Serre, C., Horcajada, P., Devic,T., Magnier, E., and Dalton, F., Effect of NH$_2$ and CF$_3$ Functionalization on the Hydrogen Sorption Properties of MOFs, Dalton Transactions, Vol. 40, No. 18, p. 4879-4881, 2011.